A Clinically Relevant, Syngeneic Model of Spontaneous, Highly Metastatic B16 Mouse Melanoma

VLADIMIR BOBEK[1,2], KATARINA KOLOSTOVA[1], DANIELA PINTEROVA[1], GRZEGORZ KACPRZAK[2], JAROSLAW ADAMIAK[3], JERZY KOLODZIEJ[2], MICHAEL BOUBELIK[1], MARTINA KUBECOVA[4] and ROBERT M. HOFFMAN[5,6]

[1]*Department of Tumor Biology, Third Faculty of Medicine, Charles University Prague, 100 34 Prague, Czech Republic;*
[2]*Department of Thoracic Surgery, Lower Silesian Centre of Lung Diseases, Medical University Wroclaw, 53-439 Wroclaw, Poland;*
[3]*Department of Pathology, Lower Silesian Centre of Lung Diseases, Grabiszynska 105, 53-439 Wroclaw, Poland;*
[4]*Radiotherapy and Oncology Clinic of Faculty Hospital Kralovske Vinohrady and Third Faculty of Medicine, Charles University Prague, 100 34 Prague, Czech Republic;*
[5]*AntiCancer, Inc, 7917 Ostrow St., San Diego, CA 92111, U.S.A.;*
[6]*Department of Surgery, University of California, San Diego, CA 92103-8220, U.S.A.*

Abstract. *We report a syngeneic model of spontaneous metastatic B16-F10 mouse melanoma in C57/BL6 mice with a very high metastatic frequency that mimics clinical metastatic melanoma. The B16 melanoma cells were injected between the skin and cartilage on the dorsal side of the ear. The model generated lymphatic and visceral metastases in all of the tested animals. In mice with large primary tumors, tumor weight correlated with the tumor growth time and also with the number of metastases in lymph nodes and organs. The dorsal ear space between the skin and cartilage enables both lymphatic and hematogenous metastatic spread. The model should be useful to study the mechanism of melanoma metastasis and to develop therapy for this currently untreatable disease.*

Several mouse melanoma models have been developed over the past few decades (1-13) and are used (i) to determine the function of particular proteins in melanoma progression; (ii) to approximate certain biological aspects of human melanomas; and (iii) to critically evaluate novel drugs. However, the main problem with these models has been their clinical relevance with respect to lymph node and visceral metastases (14). A selection of the currently available models includes (i) xenograft models; (ii) syngeneic transplantation models; and (iii) models involving genetically-modified animals. Each model has characteristic advantages which may render it more suitable for answering a respective scientific question. Syngeneic transplantation models were first established. Models such as the Harding-Passey melanoma in BALB/c·DBA/2F1 mice (15), the Cloudman S91 melanoma in DBA/2 mice (16) or the B16 melanoma in C57BL/6 mice (17, 18) have been used for approximately half a century. These model have an intact immune system. The cell lines and sublines used for generation of syngeneic models display a wide degree of heterogeneity with respect to tumor growth rate, tumor take and metastasis formation (18-20).

The syngeneic murine B16 melanoma model usually involves transplantation into the foot pad, intradermally or subcutaneously, in C57/BL6 mice (18, 21) These models usually need resection of the primary tumor, or resection of the foot pad with the primary tumor, in order for formation of distant metastases to occur (22). The second type of syngeneic melanoma model represents experimental metastases occurring following intravascular injection. Intravenous injection into the lateral tail vein is the most commonly used model resulting generally in experimental lung metastases (23). Injection into the peritoneum can generate metastatic lymph nodes (24).

Based on previously reported experiments with the syngeneic Lewis lung carcinoma metastasis model, generated by injection of the cancer cells into the ear area (25), we

Correspondence to: Vladimir Bobek, MD, Ph.D., Department of Tumor Biology, Third Faculty of Medicine Charles University, Ruska 87, 100 34 Prague, Czech Republic. E-mail: vbobek@centrum.cz

Key Words: Spontaneous metastasis, metastasis model, lymph node, B16 mouse melanoma.

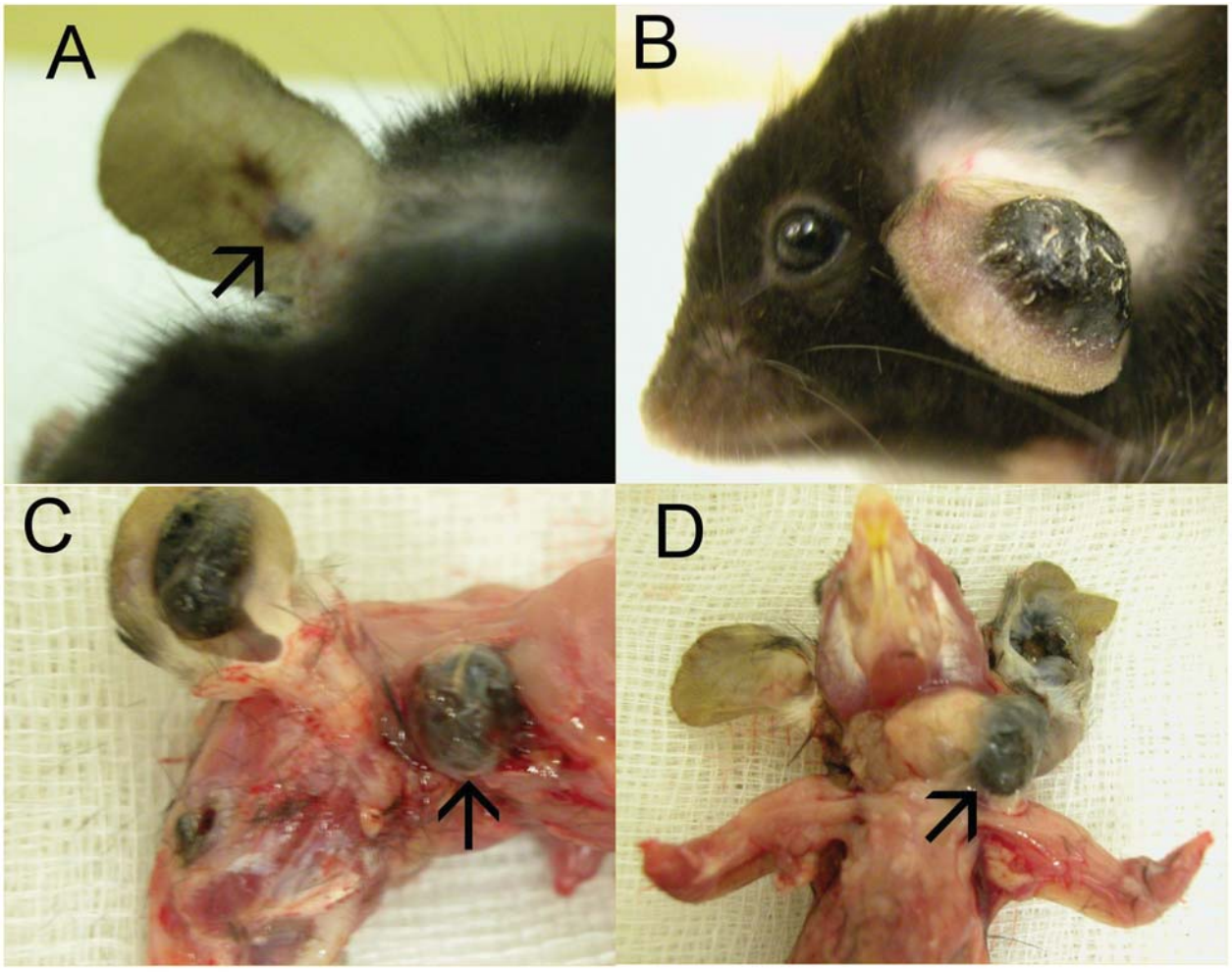

Figure 1. *Development of primary melanoma and metastasis. A: Primary melanoma ten days after transplantation. B: Advanced primary melanoma 5 weeks after transplantation. C: Lymph metastasis, sentinel node (arrow). D: Primary tumor with macroscopic metastasis (arrow) and hypertrophy of ipsilateral and contra-lateral neck, axillary and brachial lymph nodes.*

report here a syngeneic model of spontaneous highly metastatic B16-F10 mouse melanoma in C57/BL6 mice developed by injection of cancer cells between the skin and cartilage on the dorsal side of the ear. This model faithfully represents metastatic clinical melanoma.

Materials and Methods

Subcutaneous tumor growth. Three female mice (C57/BL6), 6 weeks of age, were injected subcutaneously with 2×10^6 B16 mouse melanoma cells. All of the animals were maintained in a barrier facility. All animal experiments were carried out in accordance with the Guidelines for the Care and Use of Laboratory Animals under assurance of Directive 86/609/EEC on the protection of animals used for scientific purposes in the Czech Republic.

The mouse melanoma cell line B16-F10 was obtained from AntiCancer, Inc. The cells were grown and maintained in RPMI medium, supplemented with with 10% heat-inactivated fetal bovine serum and 1% penicillin and streptomycin. The cells were first harvested from culture by trypsinisation and washed three times with cold serum-free medium before subcutaneous injection.

Ear transplantation of C57/BL6 mice. Tumors derived from *s.c.*-growing B16-F10 mouse melanoma in female mice were disassociated and a single-cell suspension in PBS was prepared. A total of 5×10^6/ml cells in 0.1 ml were injected between the skin and cartilage on the dorsal side of the ear. The female mice (C57/BL6, n=20) were anesthetized by ketamine and xylazine during transplantation.

Analysis of metastases. Mice were divided into two groups. Animals from group 1 were sacrificed 4 weeks after B16-F10 mouse melanoma cell injection (group 1: mouse numbers 1-10). The rest of the animals were sacrificed 6 weeks after the tumor cell injection (group 2: mouse numbers 11-20). The size of the

Table I. *Location of observed micro- and macro-metastases volume. Micro- and macro-metastases detected in lymph nodes and organs of the mice transplanted with B16 melanoma are described in the table below. They are shown according to the site of metastasis detection (see description of examined locations [no. 1-25] in legend). There was no metastasis detected in locations no. 17, 20, 21, 24, which correspond to heart, cerebellum, brain and kidney.*

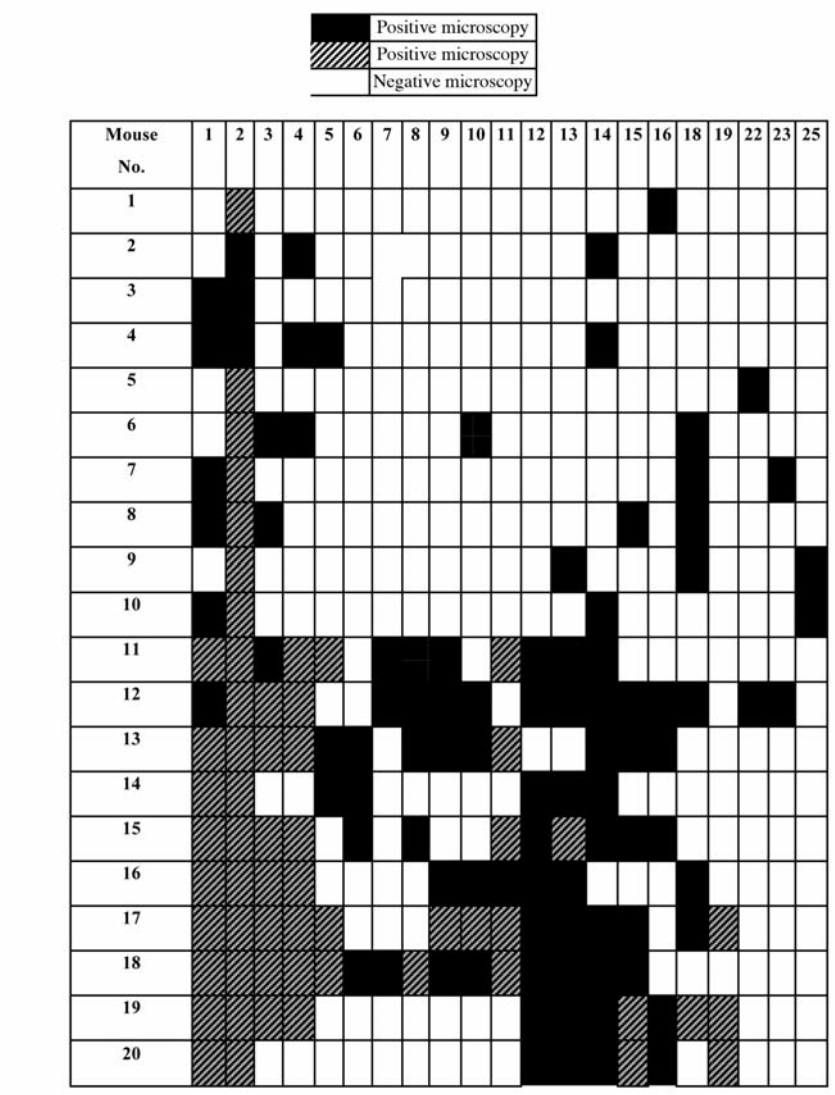

Metastatic locations of B16 melanoma after transplantation to the dorsal ear.

No.	Location	No.	Location
1	Supracervical lymph node 1	14	Axial lymph nodes
2	Supracervical lymph node 2	15	Deep cervical lymph nodes
3	Contralateral supracervical lymph node	16	Thymus + Mediastinal lymph nodes
4	Contralateral supracervical lymph node 2	17	Heart
5	Salivary gland	18	Lung
6	Contralateral salivary gland	19	Mediastinal nodes
7	Parathyroid gland	20	Cerebellum
8	Contralateral parathyroid gland	21	Brain
9-10	Thyroid gland	22	Liver
11	Brachial lymph nodes	23	Suprarenal node
12	Contralateral brachial lymph nodes	24	Kidney
13	Contralateral axial lymph nodes	25	Spleen

primary tumor was measured. The tumor volume was calculated with the formula $Tw=a(b^2)/2$, where a and b are tumor length and width (mm), respectively (13). The tissue samples from lymph nodes and organs from the neck and chest region were collected and the presence of micro- and macro-metastases was observed. At least two micro-metastatic and one macro-metastatic lesion per organ or lymph node needed to be present for an organ to be considered positive for metastasis. To detect micro-metastases, paraffin-embedded lymphoid tissue sections were stained with hematoxylin–eosin using standard procedures. The total number of metastases was correlated to tumor volume. Correlation analysis of the data was carried out using the Spearman correlation coefficient.

Results and Discussion

The number of micro- and macro-metastases observed in each mouse is shown in Table I. The total number of metastases was determined as the sum of observed micro- and macro-metastases. Tumor volume was measured four weeks after *s.c.* injection in group 1 mice and after six weeks in mice group 2 (see Figure 1 and Table I). Tumor volume correlated significantly with tumor growth time and the number of macro- and micro-metastases in lymph nodes and visceral organs (r=<0.65–0.84>; $p<0.001$), as well as with the sum of all observed metastases.

Distant micrometastases were observed in a short time (four weeks) in 100% of the transplanted animals after transplantation into the dorsal ear between the skin and cartilage. Twenty-one different metastatic sites, including lymph nodes throughout the body, were identified, similar to the Lewis lung cancer transplanted at this site (25). In the B16F10 melanoma model, cancer cells can be easily visualised due to melanin production.

The biologic mechanism of metastasis has become better understood through the study of the migration and seeding of cancer cells (26-28). The generation of visceral metastases via injection of cancer cells by subcutaneous implantation does not accurately reflect the normal sequence of events in the clinical setting in which lymph node metastasis plays a prominent role. In our study we have observed a high metastatic frequency of lymph node and visceral metastases using the dorsal site of the mouse ear for cancer-cell injection. Tumors growing at this site are drained by the lymph system.

This new metastatic melanoma model provides a valuable tool for studying the mechanisms of metastasis and for developing therapy of lymph and visceral metastases for melanoma.

Acknowledgements

This work was supported by the The Ministry of Education, Youth and Sports of Czech Republic Grant No. ME-10045, and by the Grant Agency of the ASCR, No. B501070501.

References

1 Alterman AL, Fornabaio DM and Stackpole CW: Metastatic dissemination of B16 melanoma: pattern and sequence of metastasis. J Natl Cancer Ins *75*: 691-702, 1985.

2 Brunda MJ, Luistro L, Warrier RR, Wright RB, Hubbard BR, Murphy M, Wolf SF and Gately MK: Antitumor and antimetastatic activity of interleukin 12 against murine tumors. J Exp Med *178*: 1223-1230, 1993.

3 Eberting CL, Shrayer DP, Butmarc J and Falanga V: Histologic progression of B16 F10 metastatic melanoma in C57BL/6 mice over a six week time period: distant metastases before local growth. J Dermatol *31*: 299-304, 2004.

4 Eitzman DT, Krauss JC, Shen T, Cui J and Ginsburg D: Lack of plasminogen activator inhibitor-1 effect in a transgenic mouse model of metastatic melanoma. Blood *87*: 4718-4722, 1996.

5 Fleischmann CM, Stanton GJ and Fleischmann WR Jr.: Enhanced *in vivo* sensitivity to interferon with *in vitro* resistant B16 tumor cells in mice. Cancer Immunol Immunother *39*: 148-154, 1994.

6 Deroose CM, De A, Loening AM, Chow PL, Ray P, Chatziioannou AF and Gambhir SS: Multimodality imaging of tumor xenografts and metastases in mice with combined small-animal PET, small-animal CT, and bioluminescence imaging. J Nucl Med *48(2)*: 295-303, 2007.

7 Kobayashi M, Kobayashi H, Pollard RB and Suzuki F: A pathogenic role of Th2 cells and their cytokine products on the pulmonary metastasis of murine B16 melanoma. J Immunol *160*: 5869-5873, 1998.

8 Huber MA, Kraut N, Park JE, Schubert RD, Rettig WJ, Peter RU and Garin-Chesa P: Fibroblast activation protein: differential expression and serine protease activity in reactive stromal fibroblasts of melanocytic skin tumors. J Invest Dermatol *120*: 182-188, 2003.

9 Nathanson SD, Haas GP, Mead MJ and Lee M: Spontaneous regional lymph node metastases of three variants of the B16 melanoma: relationship to primary tumor size and pulmonary metastases. J Surg Oncol *33*: 41-45, 1986.

10 Winkelmann CT, Figueroa SD, Rold TL, Volkert WA and Hoffman TJ: Microimaging characterization of a B16-F10 melanoma metastasis mouse model. Mol Imaging *5(2)*: 105-114, 2006.

11 Shiohara T, Moellmann G, Jacobson K, Kuklinska E, Ruddle NH and Lerner AB: Anti-tumor activity of class II MHC antigen-restricted cloned autoreactive T-cells. II. Novel immunotherapy of B16 melanomas by local and systemic adoptive transfer. J Immunol *138*: 1979-1986, 1987.

12 Shrayer DP, Bogaars H, Wolf SF, Hearing VJ and Wanebo HJ: A new mouse model of experimental melanoma for vaccine and lymphokine therapy. Int J Oncol *13*: 361-374, 1998.

13 Corbett T: Tumor Models in Cancer Research. Totowa, NJ: Humana Press Inc., pp. 41-71, 2002.

14 Becker JC, Houben R, Schrama D, Voigt H, Ugurel S and Reisfeld RA: Mouse models for melanoma: a personal perspective. Exp Dermatol *19(2)*: 157-164, 2010.

15 Maguire HC Jr.: Tumor immunology with particular reference to malignant melanoma. Int J Dermatol *14*: 3-11, 1975.

16 Nordlund JJ and Gershon RK: Splenic regulation of the clinical appearance of small tumors. J Immunol *114*: 1486-1490, 1975.

17 Fidler IJ, Darnell JH and Budmen MB: Tumoricidal properties of mouse macrophages activated with mediators from rat lymphocytes stimulated with concanavalin A. Cancer Res *36*: 3608-3615, 1976.
18 Fidler I J and Nicolson GL: Organ selectivity for implantation survival and growth of B16 melanoma variant tumor lines. J Natl Cancer Inst *57*: 1199-1202, 1976
19 Valle EF, Zalka AD, Groszek L and Stackpole CW: Patterning of B16 melanoma metastasis and colonization generally relates to tumor cell growth-stimulating or growth-inhibiting effects of organs and tissues. Clin Exp Metastasis *10*: 419-429, 1992.
20 Stackpole CW, Alterman AL, Braverman S and Rappaport I: Development of host immunity to phenotypically diverse B16 melanoma clones. Implications for tumor growth and metastasis. Invasion Metastasis *7*: 346-366, 1987.
21 Hoffman RM: Orthotopic metastatic mouse models for anticancer drug discovery and evaluation: a bridge to the clinic. Investigational New Drugs *17*: 343-359, 1999.
22 Price JE: Xenograft models in immunodeficient animals. In: Metastasis Research Protocols, Vol. II, Analysis of Cell Behavior *In Vitro* and *In Vivo*. Meth Mol Med. Eds: S.A. Brooks, U. Schumacher, *58*: 205-214, 2001.
23 Chirivi RG, Garofalo A, Crimmin MJ, Bawden LJ, Stoppacciaro A, Brown PD and Giavazzi R: Inhibition of the metastatic spread and growth of B16-BL6 murine melanoma by a synthetic matrix metalloproteinase inhibitor. Int J Cancer *58*: 460-464, 1994.
24 Ishibashi S, Sonoda K, Fujii K, Ishikawa K, Shiraishi N and Kitano S: A convenient murine model for the study of intra-abdominal lymph node metastasis. Oncol Rep *12(1)*: 115-118, 2004.
25 Bobek V, Kolostova K, Pinterov D, Boubelik M, Jiang P, Yang M and Hoffman RM: Syngeneic lymph-node-targeting model of green fluorescent protein-expressing Lewis lung carcinoma. Clin Exp Metastasis *21*: 705-708, 2004.
26 Yang M, Jiang P, An Z, Baranov E, Li L, Hasegawa S, Al Tuwaijri M, Chishima T, Shimada H, Moossa AR and Hoffman RM: Genetically fluorescent melanoma bone and organ metastasis models. Clin Cancer Res *5*: 3549-3559, 1999.
27 Hoffman RM: Orthotopic metastatic mouse models for anticancer drug discovery and evaluation: a bridge to the clinic. Invest New Drugs *17*: 343-359, 1999.
28 An Z, Jiang P, Wang X, Moossa AR and Hoffman RM: Development of a high metastatic orthotopic model of human renal cell carcinoma in nude mice: benefits of fragment implantation compared to cell-suspension injection. Clin Exp Metastasis *17*: 265-270, 1999.

Received September 6, 2010
Revised November 1, 2010
Accepted November 3, 2010